

Charge-order melting and magnetic phase separation in thin films of $\text{Pr}_{0.7}\text{Ca}_{0.3}\text{MnO}_3$.

Y. Q. Zhang,^{1,2} Z. D. Zhang,¹ and J. Aarts²

¹Shenyang National Laboratory for Materials Science, Institute of Metals Research, and International Center for Materials Physics, Chinese Academy of Science, 72 Wenhua Road, Shenyang 110016, People's Republic of China

²Kamerlingh Onnes Laboratory, Leiden University, 2300 RA Leiden, The Netherlands

(Received 24 February 2009; published 19 June 2009)

We investigate the effect of strain on the phenomenon of charge-order melting, that is the transformation of a charge-ordered insulating state to a metallic state under the influence of a magnetic field (the melting field) in thin films of $\text{Pr}_{0.7}\text{Ca}_{0.3}\text{MnO}_3$ grown on various substrates. We find that unstrained films grown on SrLaGaO_4 behave quite similar to bulk material, but that strained films grown on SrTiO_3 and NdGaO_3 show hugely increased melting fields. Strain relaxation by postannealing again leads to bulklike behavior. In this material the antiferromagnetic charge-order phase can coexist with a ferromagnetic insulating state. Magnetization measurements, where we demonstrate the presence of exchange bias effects, show that this is also the case in the strained films. We argue that the phase mixture in the strained films is more difficult to melt than in the unstrained case.

DOI: [10.1103/PhysRevB.79.224422](https://doi.org/10.1103/PhysRevB.79.224422)

PACS number(s): 75.47.Lx

I. INTRODUCTION

Colossal magnetoresistive manganites (CMR) are of continuing interest both from fundamental and application perspectives, because of the different electronic states which can be attained as function of carrier concentration, electric and magnetic fields, and pressure or strain. A typical compound $R_{1-x}A_x\text{MnO}_3$, with R as the trivalent rare-earth ion and A as the divalent alkali ion, is paramagnetic insulating (PI) at high temperatures and undergoes a phase transition into for instance a ferromagnetic metallic (FM) state (example $\text{La}_{0.7}\text{Ca}_{0.3}\text{MnO}_3$) or an antiferromagnetic (AF) insulating charge-order (CO) state (example $\text{Pr}_{0.5}\text{Ca}_{0.5}\text{MnO}_3$). Around the transition to the FM state, the resistance is strongly dependent on magnetic fields, and can be changed over orders of magnitude because the band formation is aided by aligning the spins on adjacent Mn ions. In the case of the insulating AF-CO state, the system can be driven into an FM state by applying (strong) magnetic fields. This so-called melting of the charge order again leads to large changes in conductivity. Since the phase transitions are driven by coupled electronic and lattice degrees of freedom, the electric and magnetic properties of these materials are easily changed by applying pressure or strain. Thin films in particular allow the possibility of investigating strain effects by growing on non-matching substrates, and thereby of strain-engineering-specific properties. An intrinsic part of the physics of CMR manganites is the phenomenon of two-phase coexistence or phase separation, which means that around and below the phase transition PI regions can coexist with FM or AF/CO regions. In essence, this is caused by the disorder which is always present in these materials. Their structures consist of oxygen octahedra in which the Mn ion is encaged and which form an almost cubic skeleton enclosing the R or A ion. The mismatch between the various ionic radii leads to rotations of the octahedra and to orthorhombic deviations from the basic cube. Disorder is then both chemical, due to the random placement of the R and A ions or oxygen vacancies, and structural, since it costs almost no energy for twinning to

occur in any of the three major cubic axes. In strained films strain relaxation is another source of disorder. Reviews on the physics of manganites as sketched above can for instance be found in Refs. 1 and 2.

In principle, charge ordering and melting are interesting phenomena to investigate in thin films, both to better understand percolation behavior and conductance switching down to nanometer scales, and to map out the effects of strain. Basically, it can be expected that in particular anisotropic strain favors a lattice-deformed charge-order state over the metallic one. Against this may work the clamping effect (the deformation coupled to the charge order is inhibited by the fixed lattice parameters of the substrate) or defects induced in the film by strain relaxation. For the system $\text{Pr}_{0.5}\text{Ca}_{0.5}\text{MnO}_3$, which shows commensurate charge order, these issues were investigated. In the bulk material, the melting fields at low temperatures are high, on the order of 25 T.³ In thin films grown on substrates with a larger lattice parameter it was shown that a competition is present between strain, which stabilizes charge order and enhances the melting fields, and disorder, which leads to lower melting fields H_m .⁴ Films with thicknesses of around 25 nm exhibit $\mu_0 H_m$ around 15 T at 20 K, somewhat lower than, but close to, the bulk value. Thicker films display lower values and also larger hysteresis between the heating and cooling branches. Forcing strain relaxation by postannealing results for an 80 nm film in a $\mu_0 H_m$ around 2 T, and no reentrance into the charge-ordered state anymore. It was also found that the charge-ordering temperature T_{CO} is significantly enhanced in strained thin films.⁵

Intrinsically lower melting fields, which are more interesting for the study and application of switching phenomena, can be found in the same system $\text{Pr}_{1-x}\text{Ca}_x\text{MnO}_3$ by changing the doping. In $\text{Pr}_{0.7}\text{Ca}_{0.3}\text{MnO}_3$, $\mu_0 H_m$ is around 2 T at 20 K, and reentrance in the charge-order state is absent.³ However, the response of the system to a magnetic field is more complicated than for the case of $x=0.5$. Instead of a single phase transition from the AF/CO state to the FM state, it was found that even for small magnetic fields, ferromagnetic but insulating (FI) clusters appear in the charge-ordered matrix,

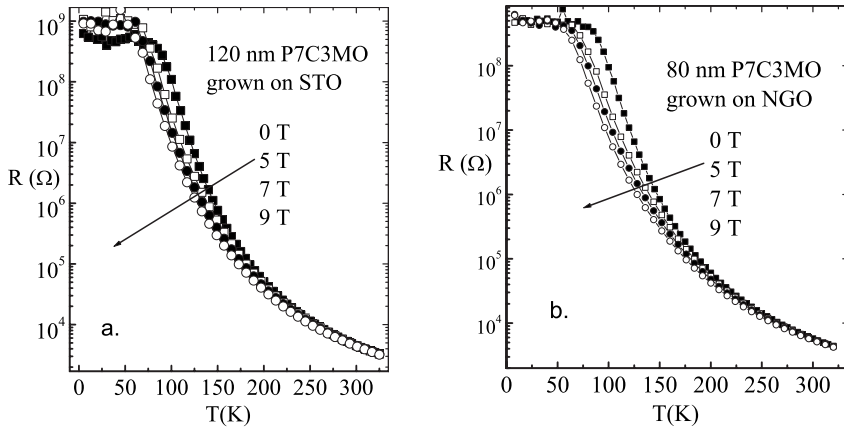


FIG. 1. Resistance R as function of temperature T in different magnetic fields as indicated for (a) a 120 nm P7C3MO thin film grown on STO and (b) an 80 nm P7C3MO grown on NGO.

which increase in size with increasing field and finally occupy the entire volume before the sample goes through an insulator-to-metal transition.^{6,7} Here we report on the behavior of thin strained films of $\text{Pr}_{0.7}\text{Ca}_{0.3}\text{MnO}_3$ (P7C3MO) grown on SrTiO_3 . Instead of finding H_m values lower than or similar to the bulk ones, we find them dramatically increased. Moreover we are able to show that, also in these films, applying a magnetic field leads to a mixture of ferromagnetic and antiferromagnetic phases, evidenced, among others, by the exchange bias phenomenon. Both effects become smaller when the film is relaxed by postannealing. Apparently, strain favors the FI state and delays the phase transition to the FM state.

II. EXPERIMENTAL DETAILS AND FILM STRUCTURE

The P7C3MO films were sputter deposited at 840 °C on SrTiO_3 (STO), NdGaO_3 (NGO), and SrLaGaO_4 (SLGO) substrates in pure oxygen atmosphere of 300 Pa with substrate source on axis geometry. The crystal structure and lattice constants were characterized by x-ray diffraction. Bulk P7C3MO crystallizes in orthorhombic ($Pnma$) structure with lattice parameters $a=0.5426$ nm, $b=0.7679$ nm, and $c=0.5478$ nm. In terms of a pseudocubic lattice parameter a_c , this means $a_c=0.3854$ nm in the a - c plane and $a_c=0.3839$ nm for the b axis. The substrates are cubic, with lattice parameters being 0.391 nm (STO), 0.386 nm (NGO), and 0.384 nm (SLGO), which means tensile strain for films on STO, and slight, respectively no strain for films on NGO and SLGO. The latter were grown for reference purposes and investigated by transport, but not magnetically. On STO, films were grown with thicknesses of 30, 80, and 120 nm. For the 120 nm film, an in-plane value was found of $a_{in}=0.3876$ nm, and an out-of-plane value was found of $a_{out}=0.3805$ nm, which means the film is still substantially strained. In order to see the effect of strain relaxation the 80 nm film was annealed for 5 h at 1000 °C in 1 bar O_2 and slowly cooled; subsequently, the values were $a_{in}=0.3848$ nm and $a_{out}=0.3823$ nm, which is close to lattice constants of bulk P7C3MO. Transport was measured on unstructured samples using a physical property measurement system (Quantum Design, USA) with maximum magnetic field of 9 T. The magnetic properties were measured with a commercial magnetometer (Quantum Design) based on a su-

perconducting quantum interference device (SQUID) with a maximum magnetic field of 5 T.

III. RESULTS AND DISCUSSION

A. Magnetotransport

Figure 1 shows resistance R versus temperature T in magnetic fields up to 9 T for the P7C3MO films with thickness 120 nm grown on STO and 80 nm on NGO. The behavior is semiconducting for all fields. The saturation at low temperatures is due to the limitation of the current source at these high resistance values. The data clearly show that for these strained films no charge-order melting takes place up to 9 T, which is surprising in view of the much lower bulk melting fields. In order to gauge the role of the strain, the 80 nm film was postannealed and an 80 nm film was grown SLGO. Figure 2 shows $R(T)$ in different magnetic fields for these two films. A transition from the insulating to the metallic state clearly starts around 5–6 T, and the metallic state is well developed at 7 and 9 T for both films. The values are higher than found in bulk, but indicate that the strain relaxation leads to lower melting fields. The conclusion of this section is that the strained films (both on STO and NGO) show strongly enhanced melting fields and that these are lowered when strain is relaxed (by postannealing) or only little strain is present (SLGO).

B. Magnetization

Next we investigate magnetic properties of the P7C3MO films grown on STO. For bulk P7C3MO, the low-temperature coexistence of ferromagnetic clusters and the charge-ordered antiferromagnetic phase was observed in two different experiments, namely, by measuring the difference between field cooled (FC) behavior and zero-field-cooled (ZFC) behavior and by measuring the hysteresis loops in magnetization versus applied field. For bulk material it was found that the ZFC and FC magnetization curves are different at low temperatures and merge at a temperature we call the irreversibility temperature T_{irr} . The measurement procedure is as follows. The film was first cooled in zero field to 5 K. Then a magnetic field of 10 mT was applied and the magnetization was measured while warming to room temperature. This constitutes the ZFC magnetization curve. The

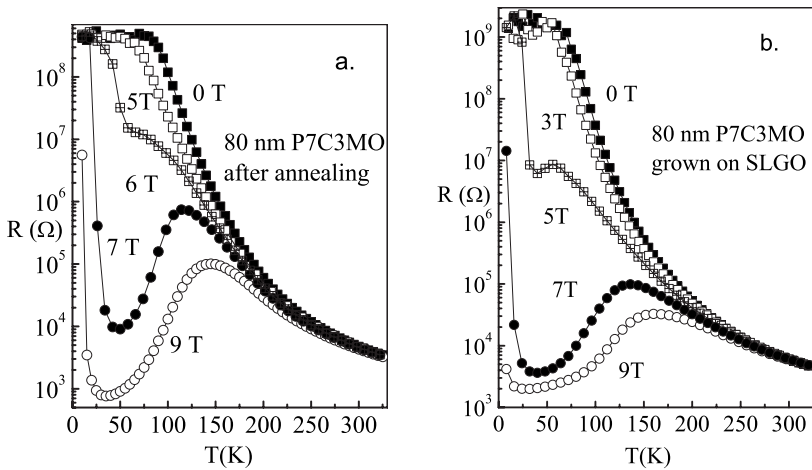


FIG. 2. Resistance R as function of temperature T in different magnetic fields as indicated for (a) an 80 nm P7C3MO thin film grown on STO after annealing at 1000 °C for 5 h and (b) an 80 nm P7C3MO thin film grown on SLGO.

FC magnetization was then measured by cooling to 5 K in the same field. Figure 3 shows the ZFC and FC magnetizations as a function of temperature in the applied field of 10 mT for the 30, 80, and 120 nm P7C3MO film grown on STO. A conspicuous difference is observed between the ZFC and FC magnetizations, with T_{irr} values of 61 K (30 nm), 51 K (80 nm), 50 K (120 nm), and 46 K (80 nm after annealing; see inset in Fig. 3). The reduction in T_{irr} upon annealing is small, but reversibility is also not complete even up to room temperature. The annealed and partly strain relaxed film appears to have a larger size distribution of ferromagnetic clusters. Also important is the value of the magnetization in the FC experiments, which is on the order of $0.2\mu_B/\text{Mn}$ atom for the 30 nm film. This will be discussed below.

In the previous paragraph we showed that all P7C3MO films grown on STO exhibit insulating behavior even in a magnetic field of 9 T. Together with the magnetization measurements, this suggests that in essentially the whole field range there may be coexistence of the inhomogeneous CO-AF phase and clusters of the FI phase, in other words, ferromagnetic clusters dispersed in an antiferromagnetic matrix. That the material is ferromagnetic can be checked by measuring magnetic hysteresis loops, but with a mixture of F

and AF material, also an exchange bias effect might be expected. In the somewhat similar system $(\text{La,Sr})\text{CoO}_3$, exchange bias was found in a phase-separated system,⁸ although in that case the mixture is between a ferromagnetic and a spin-glass phase. We measured hysteresis loops for the 30 and 120 nm films on STO by cooling them in a magnetic field of 0.3 T from 300 to 30 K, which is below T_{irr} for both films. This was performed for different ranges of the applied field (the maximum field used for measuring the loop) $\mu_0 H_{a,max}$, namely, $\pm 0.3, \pm 1.5, \pm 2.5, \pm 3.5,$ and ± 5.0 T. An example is given in Fig. 4 for the 30 nm film. We find a clear exchange bias H_E manifesting itself as a shift in the hysteresis loop along the field axis and defined as $H_E = (H_c^+ + H_c^-)/2$, where H_c^{\pm} are the coercive fields for positive and negative applied fields. The values are around 5 mT for the small-ranged loops and decrease with increasing loop range $H_{a,max}$, as shown in Fig. 5(a). While the presence of an exchange bias confirms that a mixture of F and AF phases is present in the film, the decrease suggests that with increasing field the ferromagnetic phase expands at the expense of the

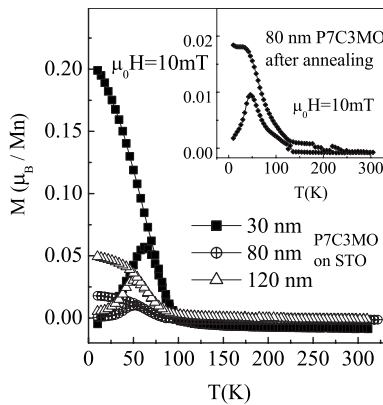


FIG. 3. The temperature dependence of the ZFC and FC magnetizations measured in a field of 10 mT for the 30, 80, and 120 nm P7C3MO films grown on STO. Inset: ZFC and FC magnetizations as a function of temperature in a field of 10 mT for an annealed 80 nm P7C3MO film.

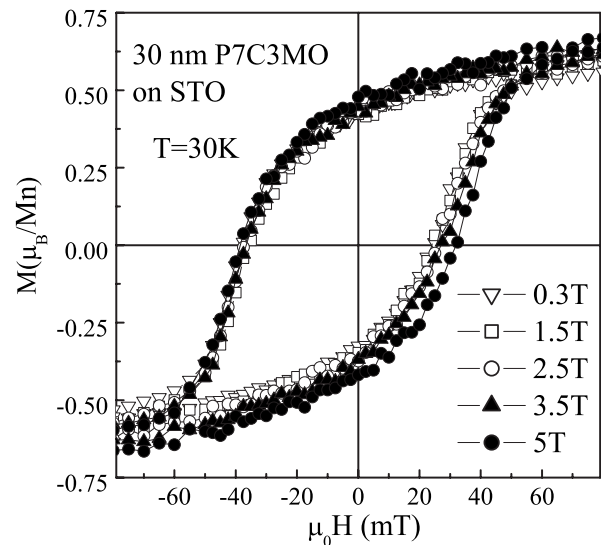


FIG. 4. Hysteresis loops of a 30 nm P7C3MO film grown on STO measured at 30 K with the maximum applied field in the range $\pm 0.3, \pm 1.5, \pm 2.5, \pm 3.5,$ and ± 5 T, after cooling in a field of 0.3 T.

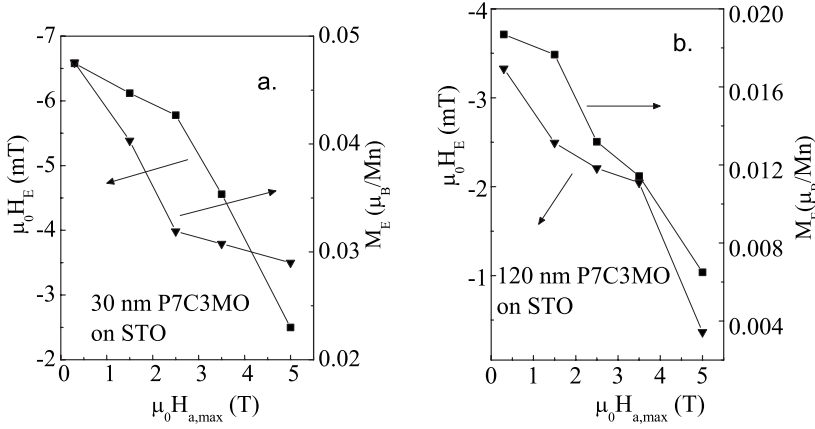


FIG. 5. The dependence of the horizontal loop shift $\mu_0 H_E$ and the vertical loop shift M_E on the maximum applied field $\mu_0 H_{a,max}$ for (a) a 30 nm P7C3MO film grown on STO and (b) a 120 nm P7C3MO film grown on STO, measured at 30 K after cooling in a field of 0.3 T.

AF/CO phase, leading to a decrease in the amount of interface.

The value of the saturation magnetization for the 30 nm film is around $0.6\mu_B/\text{Mn}$ atom, significantly increased from the value found in field cooling in 10 mT. Moreover, apart from a shift in coercive fields, we also find a shift in the loop along the magnetization axis which we call M_E , defined as $M_E = (M_R^+ + M_R^-)/2$, where M_R^{\pm} is the positive (negative) remanent magnetization in zero field. Note that positive here is defined with respect to the direction of the cooling field. The value for M_E is around 10% of the saturation magnetization, and this value also decreases with increasing loop range, as shown in Fig. 5(a). Loop shifts are well-known phenomena in F/AF mixtures or bilayers.⁹ In our case, we conclude that for the small applied cooling fields the interfacial energy between the AF phase and the F clusters wins from the effective Zeeman energy of the clusters in the applied field, which leads to pinning of the magnetization direction of the clusters and the observed positive shift. Increasing the applied field in the loop does not change the volume of ferromagnetic material, as is apparent from the similar values of the saturation magnetization, but it probably leads to a larger connected volume and therefore to a decrease in interface between clusters and AF matrix. The magnetization pinning becomes less effective, and the positive loop shift decreases. In addition, we observe that the absolute value of the exchange bias observed in the 120 nm film is smaller than in the 30 nm film under the same cooling fields, which we assume is due to the strain relaxation and correlated with the effect on the irreversibility temperature.

IV. DISCUSSION

Summarizing the results, we find clear evidence for the formation of a field-induced ferromagnetic insulating state similar to what was found in bulk material. We assume that, as in the bulk, the FI state forms at small applied fields in the form of FI clusters, increasing in size with increasing applied field. As a consequence, both horizontal (exchange bias) and vertical (magnetization) loop shifts are found. In the 30 nm

film, the increase in ferromagnetic volume is clear from the change of $0.2\mu_B/\text{Mn}$ atom in a field of 10 mT to $0.6\mu_B/\text{Mn}$ atom in a field of 0.3 T and $1.1\mu_B/\text{Mn}$ atom in 5 T (not shown). In investigations on bulk material,⁷ values were quoted for the magnetic moment of the FI phase [called the reverse orbital order (ROO) phase] of $0.8\mu_B/\text{Mn}$ atom and the volume fraction in zero field cooling of about 50%. It was also found that the transition to the FM state occurs above 5 T, with an essentially full moment of $3.5\mu_B/\text{Mn}$ atom in 7 T. Furthermore, it was found in Ref. 6 that the transformation to 100% FI phase is complete around 0.5 T. In our case of strained thin films such as the 30 nm one, we find qualitatively similar, but quantitatively very different behavior. The data indicate a smaller fraction of FI phase upon low-field cooling, and an incomplete transformation in fields up to 5 T. This is seen both in the value of the saturation magnetization, and in the fact that exchange bias is still observed in these fields. It is reasonable to conclude that the strain is responsible for this change in behavior. In Ref. 7 it was suggested that intragranular strain could be the origin for coexistence of both phases of the CO and ROO phases. In our case, strain apparently strongly hinders the transformation to the ROO phase, leading to a phase mixture, which, in turn, is more difficult to transform to the metallic state. The fact that strained thin films of $\text{Pr}_{0.7}\text{Ca}_{0.3}\text{MnO}_3$ show significantly higher melting fields than the bulk material, even up to quite large thickness and in strong contrast with earlier findings on $\text{Pr}_{0.5}\text{Ca}_{0.5}\text{MnO}_3$, is connected to the intermediate phase which is present in the case of $\text{Pr}_{0.7}\text{Ca}_{0.3}\text{MnO}_3$.

ACKNOWLEDGMENTS

This work has been carried out in a collaborative research Project No. 04CDP020 under the auspices of the Dutch Royal Academy of Sciences (KNAW) and the Chinese Academy of Sciences and was also supported by the National Natural Science Foundation of China under Grant No. 50331030. We would also like to acknowledge R. Hendrikx and M. Hesselberth for assistance in the sample preparation and characterization.

- ¹E. Dagotto, T. Hotta, and A. Moreo, *Phys. Rep.* **344**, 1 (2001).
- ²M. B. Salamon and M. Jaime, *Rev. Mod. Phys.* **73**, 583 (2001).
- ³Y. Tomioka, A. Asamitsu, H. Kuwahara, Y. Moritomo, and Y. Tokura, *Phys. Rev. B* **53**, R1689 (1996).
- ⁴Z. Q. Yang and R. W. A. Hendrikx, P. J. M. v. Bentum, and J. Aarts, *Europhys. Lett.* **58**, 864 (2002).
- ⁵Z. Q. Yang, Y. Q. Zhang, J. Aarts, M.-Y. Wu, and H. W. Zandbergen, *Appl. Phys. Lett.* **88**, 072507 (2006).
- ⁶I. G. Deac, J. F. Mitchell, and P. Schiffer, *Phys. Rev. B* **63**, 172408 (2001).
- ⁷P. G. Radaelli, R. M. Ibberson, D. N. Argyriou, H. Casalta, K. H. Andersen, S.-W. Cheong, and J. F. Mitchell, *Phys. Rev. B* **63**, 172419 (2001).
- ⁸Y. K. Tang, Y. Sun, and Z. H. Cheng, *Phys. Rev. B* **73**, 174419 (2006).
- ⁹J. Nogués, C. Leighton, and I. K. Schuller, *Phys. Rev. B* **61**, 1315 (2000).